Reconstruction of trophic state shifts over the past 90 years in a eutrophicated lake in western Switzerland, inferred from the sedimentary record of photosynthetic pigments

Stamatina Makri[1, 2], Andrea Lami[3], Brigitte Lods-Crozet[4], Jean-Luc Loizeau[1]

1. Department F.-A. Forel for Environmental and Aquatic Sciences & Institute of Environmental Sciences, University of Geneva, 66 Carl-Vogt Boulevard, CH-1211 Geneva 4, Switzerland
2. Institute of Geography & Oeschger Centre for Climate Change Research, University of Bern, Erlachstrasse 9a, CH-3012 Bern, Switzerland
3. Institute of Ecosystem Study (ISE-CNR), 50 Largo Tonolli, 28922 Verbania Pallanza, Italy
4. Direction Générale de l'Environnement – Division Protection des eaux, 155 Ch. des Boveresses, CH-1066 Epalignes, Switzerland

Corresponding author

Stamatina Makri

Institute of Geography & Oeschger Centre for Climate Change Research

University of Bern

Erlachstrasse 9a, CH-3012 Bern, Switzerland

E-mail: stamatina.makri@giub.unibe.ch

Co-authors

Dr. Andrea Lami E-mail: a.lami@ise.cnr.it

Dr. Brigitte Lods-Crozet E-mail: brigitte.lods-crozet@vd.ch

Dr. Jean-Luc Loizeau E-mail : jean-luc.loizeau@unige.ch

Keywords

Phytoplankton community composition, Cyanobacteria, Global change, Re-oligotrophication, Paleolimnology, HPLC

This is a post-peer-review, pre-copyedit version of an article published in the Journal of Paleolimnology. The final authenticated version is available online at: http://doi.org/10.1007/s10933-018-0049-5.

Abstract

Anthropogenic eutrophication can initiate vast and persistent ecosystem state changes in lakes. Such changes may be characterized by increased phytoplankton taxa variability, which can affect the effectiveness and time of lake recovery mechanisms.

Lake Morat in Switzerland has undergone intense eutrophication in the 20th century (phosphorous concentrations up to 150 μg L^{-1}) caused by excessive nutrient loadings from agricultural intensification and urbanization. Phosphorous reduction measures since 1986, such as the ban of phosphates in detergents and decreased use of fertilizers in agriculture, have resulted in total phosphorous concentrations up to 20 μg L^{-1} today. Despite this drastic reduction of total phosphorous, total biomass production stays high. We investigate historical changes in the phytoplankton community during the eutrophication and re-oligotrophication periods by comparing historical limnological data with sediment pigment concentrations measured by HPLC and other geochemical proxies in a radiodated sediment core.

For the last 90 years, we identified four major trophic state changes in Lake Morat. The first period (AD 1924-1937) is characterized by low pigment concentrations and nutrient inputs, with good oxygen conditions. This section represents trophic conditions before the intensive eutrophication phase. The second period (AD 1937-1970) revealed an abrupt increase in pigment concentrations with higher primary production, cyanobacteria dominance and reduced oxygen levels. Oscillaxanthin indicated a *Planktothrix rubescens* dominance (AD 1954-1970) with concentrations up to 800 nmol g^{-1} OM. Their decline after AD 1970 suggests the initiation of an intense eutrophication phase (AD 1970-1983) associated with the dominance of other cyanobacteria species, higher total phosphorous inputs, and intense anoxia. In the restoration period (AD 1983-2014), there was a shift in the phototrophic community from cyanobacteria to green algae dominance, yet some cyanobacteria species remain present.

Rapid phytoplankton community changes were identified in the studied period, yet overall primary production response was low. Limnological data revealed a delay of phosphorous reduction due to phosphorous recycling from the sediments. The observation of complex lake ecosystem reactions to prolonged eutrophication and subsequent re-oligotrophication, as shown by the paleolimnological and limnological data in this study, emphasize the importance of careful lake management to revert eutrophication back to historical reference biomass values.

Introduction

During the 20th century, increased anthropogenic impacts caused intensive ecosystem disturbances, excessive growth of primary production, changes in algal communities and anoxia for most lakes under local anthropization (Jenny et al. 2016). Extensive increase of nutrient levels results in large scale changes in lake conditions, leading to irreversible tipping point transitions in many cases (Scheffer et al. 2001; Scheffer and Carpenter 2003). Combining paleolimnology and contemporary limnological parameters creates a powerful approach to assess long-term shifts and identify key ecosystem components, such as phytoplankton abundance changes (Battarbee et al. 2005; Smol 2010). Pressures such as eutrophication cause several complex responses in lake systems, making it extremely difficult to understand all interactions involved. These can include biomass shifts, taxonomic algal community changes, oxygen level and nutrient cycle fluctuations (Smith and Schindler 2009). Multi-proxy sediment records can be used to test ecological theories of sudden ecosystem state changes in the past, and also evaluate the conditions of these states (Cottingham et al. 2000). In particular, sedimentary pigment records can be used to reconstruct overall primary production and phototrophic distribution of past communities (Guilizzoni et al. 1983; Lami et al. 2000). This method is effective because pigments are present in all autotrophic organisms and are specific to particular classes of algae (Leavitt 1993).

Anthropogenic eutrophication remains a crucial threat to lakes despite more than 50 years of research (Schindler 2006). To improve the ecological quality of lakes, major efforts have been made, especially to decrease external nutrient loading (Mardsen 1989; Sas 1989). However, studies have shown that there is a large range of lake responses to re-oligotrophication that remain poorly understood (Carpenter et al. 1999; Anderson et al. 2005; Jeppesen et al. 2005). Investigating individual lake systems is particularly important to understand re-oligotrophication mechanisms, since every lake has the potential to give specific responses thanks to its unique characteristics.

Lake Morat (Switzerland), which is naturally mesotrophic (Davaud 1976), underwent strong eutrophication during the past century, with total phosphorus concentrations up to 150 $\mu g\ L^{-1}$ in 1982 (Liechti 1994). Since 1986, an intense effort to cut anthropogenic phosphorus inputs has drastically reduced phosphorus concentrations to 18 $\mu g\ L^{-1}$ today (BENEFRI 2017). However, despite this reduction, primary production remains high and an anoxic hypolimnion develops each summer. To infer phytoplankton communities' shifts within the eutrophication and re-oligotrophication periods, we reconstructed Lake Morat's historical

phototrophic community development. We did so by using a sedimentary record of pigments and geochemical parameters, combined with contemporary limnological data. Specifically, we aim to identify historical changes in phytoplankton abundance, and examine possible factors that influence primary production, which remains persistently high despite restoration measures.

Study area

Lake Morat is located in the western part of the Swiss Plateau at the foot of the first range of the Jura Mountains at 429 m a.s.l., in north-west Switzerland (46°56'N, 7°5' E) (Fig. 1). Its total surface area is 22.8 km^2 and its maximum depth reaches 45 m. It is an exoreic, meso-eutrophic, monomictic lake, with pronounced seasonal stratification and a residence time of 1.6 years (Table 1). Studies have also shown the development of an anoxic hypolimnion each summer (Müller and Schmid 2009). The increased organic matter production and flat morphology of lake bottom, coupled with the relatively small oxygen reservoir (average depth of 23.3 m) create an anoxic hypolimnion below 10 m depth during summer stratification. The lake is of glacial origin, formed in the Early Holocene (11.7 k yr BP) after the last glacial retreat (Davaud 1976). It sits on the Lowland Molasse, as well as most of its catchment area. The lake occupies a low depression of the Broye River plain, which is its main tributary. The Broye River flows into Lake Morat at the SW and outflows at the NW connecting the lake with Lake Neuchatel. The catchment area (713 km^2) is limited in the NW by the slopes of Mont Vully, but its vast part lies below 1'000 m a.s.l. The land use of the catchment is mainly agricultural, covered with low vegetation and croplands (Fig. 1). The climate of the region is temperate with mean annual temperature of ~8 °C and mean annual precipitation of ~1040 mm (Payerne station). The natural vegetation on the area consists of deciduous forest (Magny et al. 2005).

During the last 150 years, Lake Morat and the area around it has undergone vast hydrological changes with important consequences for its ecological status. First observations of early eutrophication started already in 1825, by seasonal observation of *Planktothrix rubescens* by de Candolle (Liechti 1994). Recurrent flooding of cultivated areas led to extensive water correction works. The first in 1868-1891, drained the surrounding area by diverting the Aar River and balanced water levels of the three connected lakes (Biel, Neuchatel and Morat). In 1935, the lake was described as mesotrophic with abundant biomass, phosphorous levels of ~10-15 $\mu g\ L^{-1}$, and oxygen content of 1 $mg\ L^{-1}$ at 40 m in the

end of summer (oxygen saturation from 56.5 % at 10 m to 7.3 % at 40 m depth) (Rivier 1936). In 1939, an additional dam was constructed at the Nidau-Buren canal in Port, downstream of Lake Morat. In 1955, phosphorous levels were of 35 μg L^{-1}, with oxygen content lower than 4 mg L^{-1} during stratification (EAWAG 1960). The second Jura water correction works (1962–1973), aimed to reduce lake levels variations by deepening the existing canals. Since then all three lakes (Morat, Neuchatel, and Biel) form a reservoir in order to retain water overflow from the Aar River, which flows directly into Lake Biel. These interventions gradually resulted in the release of a vast area for agricultural use. Extensive agriculture culminating after 1960, resulted in a phase of high nutrients inputs (reaching up to 150 μg L^{-1} of P in 1982) and intense eutrophication with bottom water oxygen concentration lower than 1 mg L^{-1} at the end of summer (oxygen saturation less than 8 %) (Liechti 1994). From 1962 to 1996, 32 Wastewater Treatment Plants (WWTP) were built in the watershed. In 1975, there was an installation of a WWTP that discharges its waters directly into Lake Morat (BENEFRI 2017). In 1986, restoration measures taken for reducing phosphorous inputs, ban of phosphates in detergents and decreased use of fertilizers in agriculture initiated the process of re-oligotrophication. However, algal biomass remains high until today, with persistent anoxia during stratification (BENEFRI 2017).

Materials and methods

Sediment analysis

Two parallel UWITEC gravity cores were retrieved in July 2014, at 43 m depth of Lake Morat (Fig. 1). Volume magnetic susceptibility (VMS) was measured in both cores prior to opening using a Bartington MS2 susceptibilimeter. Core M3 (54.5 cm length) was sub-sampled every 1 cm and analyzed for water content, grain size, loss on ignition (LOI), C/N ratio, ^{137}Cs and ^{210}Pb activities and pigment quantification by HPLC. M1 (48 cm length) was used for XRF scanning. Sediment description was based on visual criteria, as well as on carbon, grain size, carbonate content and magnetic susceptibility (Schnurrenberger et al. 2003).

Sediment grain size distribution was measured with a Coulter LS-100 laser diffraction analyzer (Loizeau et al. 1994). We measured organic matter and carbonate minerals by sequential LOI, and calculated total organic (Corg) and inorganic carbon (Cinorg) using previous published equations (Dean 1974; Heiri et al. 2001). A CN Perkin Elmer 2400

Analyzer measured total nitrogen (N) for all M3 samples. Corg/N ratio was used to determine organic matter (OM) origin. Fresh OM from planktonic organisms has a C/N ratio of 6 to 9, whereas terrestrial plants have ratios higher than 15 (Meyers and Benson 1988).

XRF core scanning was made with an AVAATECH X-ray scanner at the University of Bern. For lighter elements (Al, Si, Cl, K, Ca, Ti, Ba) we used a Cr-tube of 10 kV voltage. For heavier elements (Mn, Fe, Ni, Cu, Zn, Br, Sr) we used a Mo-tube of 40 kV voltage. For both measurements, a 2 mm resolution and 10-second exposure time were applied. The results are expressed as counts per second (cps) and have a semi-quantitative character for the abundances of different elements. For the interpretation of the results, K and Ti were used as proxies of detrital inputs to the lake (Koinig et al. 2003). Their correlation with Si can give evidence for allochthonous versus autochthonous inputs of this element in the lake. Since XRF data were not normally distributed, relationships between elements were assessed by a Spearman's rank correlation test run in R (R Core Team 2015). Probability values (p-values) were calculated from the number of degrees of freedom (DF) and corrected for autocorrelation (von Gunten et al. 2012) .

To construct a chronology for the first 45.5 cm of M3, we measured specific gamma activities of ^{210}Pb, ^{214}Pb, ^{137}Cs and ^{7}Be using an HPGe ORTEC detector at 1 cm resolution. To calculate the numerical dates, we used the constant-rate-of-supply (CRS) model (Appleby 2001). The model was constrained by using ^{137}Cs peak activities, which provided independent age markers from the fallout of atmospheric nuclear bomb testing, starting in AD 1953 and culminating in AD 1963, as well as the Chernobyl accident (AD 1986). For the missing part of unsupported ^{210}Pb measurements (46.5-54.5 cm), dates were assessed by linear extrapolation of calculated dates. The missing inventory of unsupported ^{210}Pb was calculated by extrapolation from the exponential regression of the unsupported activities and cumulative dry mass. The completeness of the coring was assessed by the measurement in the core top of ^{7}Be, a short-lived radionuclide produced in the stratosphere by the interaction of cosmic rays with atmospheric molecules, and transported to the Earth surface mainly through wet deposition (Kaste et al. 2002).

Due to the labile nature of pigments, samples used for pigment analysis were treated and protected from light exposure and high temperatures (Leavitt 1993). After sediment subsampling, all 54 samples from M3 were deep frozen (at -20°C). We used 0.5-1 g of fresh wet sediment and extracted pigments overnight at 4°C under nitrogen with 90% acetone (Lami et al. 2000). The suspension was centrifuged at 3000 rpm for 10 minutes and washed with additional 90% acetone aliquot to obtain a clear extract. We used a spectrophotometer

(SAFAS, UVmc2) to analyze the supernatant for chlorophylls, chlorophyll derivatives (CD) and total carotenoids (TC). Single chlorophylls and carotenoids were determined by reverse-phase HPLC (Mantoura and Llewellyn 1983). For this, we used a dual channel variable wavelength UV-VIS DAD detector, set at 460 nm and 656 nm for carotenoids and chloropigments, respectively. Results were corrected using water content measurements. Chlorophyll derivatives were expressed as spectrophotometric units per gram of organic matter (U g^{-1} OM) and total carotenoids as milligrams per gram of organic matter (mg g^{-1} OM). Single pigments and single carotenoids were expressed as nanomoles per gram of organic matter (nmol g^{-1} OM). This was done to avoid dilution effects of clastic material from the catchment (Guilizzoni et al. 1983; Lami et al. 1994).

To evaluate changes in the phototrophic community composition, we selected pigment proxies according to their taxa affiliation (Leavitt and Hodgson 2001; Guilizzoni and Lami 2002; Roy et al. 2011). Chl α (found in most algae and plants), β carotene (found in most algae, plants and some phototrophic bacteria) and pheophytin α (Chl α derivative) are valuable indicators of total algal biomass. Chl *b*, lutein and violaxanthin are found in chlorophytes and euglenophytes. Pheophorbide α (Chl α derivatives) occurs in senescent algae and indicates zooplankton grazing. Diadinoxanthin and diatoxanthin are elements of the xanthophyll cycle in the chromophyte algae and along with fucoxanthin are mainly associated with diatoms, dinoflagellates and chrysophytes. Certain dinoflagellate contain peridin as a dominant pigment, however it is not common in the fossil record since it is a very labile compound. Alloxanthin is associated to cryptophytes. Echinenone and zeaxanthin are attributed to various cyanobacteria, while myxoxanthophyll, myxol-2'-1 and cantaxanthin are common in colonial cyanobacteria. Oscillaxanthin characterizes *Oscillatoria rubescens* and *Athrospira sp*. (Hertzberg et al. 1971), however only *P. rubescens* has systematically been observed in the lake. Astaxanthin is associated with herbivores, which indicate zooplankton abundance.

With respect to pigment ratios, pigment degradation processes are different for chlorophylls and carotenoids. Under high oxygen conditions, chlorophylls degrade more easily into their degradation, while carotenoids are more stable (Leavitt and Hodgson 2001). Under low oxygen conditions, more chlorophyll than its derivatives should be present in the sediments (Yacobi et al. 1991). The ratio of 430:410 is a reliable proxy of pigment degradation, because it depicts the different wavelength absorptions between Chl α (absorption at 430 nm) and its degradation product pheophytin (absorption at 410 nm) (Guilizzoni et al. 1992). Thus, low oxygen levels would result in a higher ratio. The CD/TC

ratio (chlorophyll derivatives/total carotenoids) can also serve as an index of changes in lake trophic status as blue-green algae, which usually dominate nutrient-rich eutrophic lakes, are rich in carotenoids and thus lower the ratio (Guilizzoni and Lami 2002).

To evaluate pigment stratigraphy results and define shifts in lake trophic state, we conducted a principal component analysis (PCA) and constrained hierarchical clustering (CONISS) in R, which used both chlorophylls and carotenoids. We computed a Bray and Curtis dissimilarity matrix by using the "vegan" package and then proceeded to constrained hierarchical clustering by using "rioja". For PCA, we again used tools provided by the "vegan" package in R (Oksanen et al. 2017).

Limnological data

Lake Morat has been monitored by the BENEFRI group since 1986 (BENEFRI 2017). Datasets from each May and October from 1986 to 2014 were analyzed for selected variables such as oxygen, total phosphorous (TP), dissolved inorganic phosphorous (DIP), dissolved inorganic nitrogen (DIN) and the resulting DIN/TP ratio in epilimnion and hypolimnion. Water samples were taken every 5 m in the epilimnion and every 10 m in the hypolimnion. In addition, we examined variations in the vertical distribution of dissolved oxygen and temperature in 2005 during the main seasonal phases of the lake. This is during spring turnover (normally expected at the end of February in Lake Morat), at the peak and end of the stratification period in August and October, respectively. The aim of the limnological data analysis is to distinguish shifts in nutrient and oxygen availabilities and their connection with observed changes in phototrophic communities during the restoration period.

Results

Sedimentology and geochemistry

Fig. 2 summarizes the sedimentological and geochemical proxy data. Core-to-core correlation suggests similar depositional conditions with an average offset of 1-1.5 cm possibly due to sediment compaction. The sediment sequence consists mainly of clayey silt and mud in the upper part of the sequence. Overall Corg concentration ranges from 3.1 % to 5.6 % and N concentration ranges from 0.23 to 0.54 %, both showing an increasing trend upwards in the core. Cinorg follows a quite stable distribution, with values from 4.7 to 7.7%. The Corg/N

ratio ranges from 10 to 14. It never exceeds the limit of 15 for terrestrial dominance of OM origin nor drops below 10, which would indicate that autochthonous aquatic OM is dominant. OM sources are thus of mixed allochthonous and autochthonous origin. Raw XRF element counts show no large variations, which suggests a rather homogenous sediment chemical composition. Correlation significance levels revealed a very strong positive correlation between K and Ti (r_s = 0.9, p-value<0.001). Fe correlated strongly with Ti (r_s = 0.75, p-value<0.001) and K (r_s = 0.7, p-value<0.001). Si did not show any significant correlation with K and Ti suggesting that autochthonous sources of biogenic silica dominate the Si record.

Color variations are apparent. Starting from the bottom, from 54.5 cm to 46 cm sediments consist of light brownish gray clayey silt, with diffuse millimetric dark greyish brown laminae. From 46 cm to 35 cm, sediments consist of olive brown clayey silt with diffuse dark olive brown laminae. VMS does not show any large variations in these bottom two parts and keeps a rather stable value. From 35 to 16 cm, sediments are composed of dark olive brown silt, with blurred olive brown laminae. VMS shows a gradual increase in this section. The most distinct section in terms of sediment structure and physicochemical conditions is the upper part of the core, from 16 cm to surface. In this part, we observe well-preserved lamination. Sediments consist of alternating laminae of light olive-brown and dark-olive brown mud. Approximately 25 laminae appear in the top 16 cm. Corg concentrations start to steadily exceed the mean values with some fluctuations, and reach a peak at the top of the core. For this upper part, Corg values range from 4.0 to 5.64 %, while values found in the lowest part range from 3.0 to 3.5 %. N values also start exceeding the mean from 16 cm to the top. VMS increases significantly from 16 to 4 cm, which suggests a stronger presence of ferromagnetic materials. Cinorg values are below the mean in this part (overall range from 4.7 to 7.7 %) showing a minimum of 4.7 % at 8 cm, suggesting less presence of diamagnetic biogenic material, which correlates with high VMS.

Chronology

Fig. 3 presents the activity profiles of ^{210}Pb (total and unsupported) and ^{137}Cs, as well as the CRS model ages. The core integrity is verified by the presence in the top centimeter of ^{7}Be with an activity of 45.8 Bq kg^{-1}. Unsupported ^{210}Pb activity shows a typical exponential decline profile, whereas supported activity of ^{214}Pb stays rather constant.^{137}Cs profile shows two distinctive peaks at 30 cm (60.4 Bq kg^{-1}) and at 16 cm (104.5 Bq kg^{-1}), which indicates the two major fallout events of AD 1963 and AD 1986 respectively. We can also see the first

radioactive signal of ^{137}Cs in the sediments at 37 cm (AD 1953). The peak of AD 1986 serves as a chrono-marker to constrain our CRS model. The model is also able to fit the other two chrono-markers on the profile, with an offset of ±2 years. From the CRS model, the average sedimentation rate is calculated to be 0.33 g cm^{-2} $year^{-1}$ with no large variations. This along with the activity profile of unsupported Pb indicate a constant sediment accumulation background.

Laminae are only visible in the upper part of the core, from 16 cm to the surface. For the top 16 cm of the core, 25 laminations are counted. From the CRS model, the calculated deposition date for the 16 cm sediment layer is AD 1986-87 (approximately 27 years before coring), which suggests varve formation, probably associated with a transition to a different trophic level in this section.

Pigment stratigraphy

Fig. 4 presents the four distinct zones of sedimentary pigment shifts. Zone boundaries were defined based on PCA output and clustering dendrogram (Fig. 5). The PCA bi-plot shows the expression of our sample data in terms of the principal components. Most of our data are distributed along PC1, which explains 50.2 % of the total variance. In the plot, we observe four groups of similar scores in different colors, which correspond to the four clusters of the clustering dendrogram.

The first group of PC1 scores corresponds to samples from 55 to 48 cm (Zone I), with low scores for all variables (Fig. 5). This zone records the lowest concentrations for all pigments. Based on the specific carotenoids, we assume the presence mainly of green algae such as chlorophytes and euglenophytes (lutein), chromophyte algae such as diatoms, dinoflagellates, crysophytes (diadinoxanthin), as well as less abundant cyanobacteria (echinenone, zeaxanthin) and few colonial forms (cantaxanthin) (Fig. 4a). CD/TC ratio shows an increasing trend, while 430:410 shows a decreasing trend with minimum values overall (Fig. 4b).

The second group of PC1 scores, with samples from 48 to 27 cm (Zone II), separates higher scores for myxoxanthophyll, myxol-2'-1, echinenone and oscillaxanthin, which indicate *Oscillatoria* and other colonial and filamentous cyanobacteria species (Fig. 5). This zone is characterized by a general increase in pigment concentrations. Chl α, chlorophyll derivatives, and carotenoids specific to green algae species (lutein), diatoms (diatoxanthin, diadinoxanthin) and cryptophytes (alloxanthin) all increase in this zone (Fig. 4a). There is also

a significant increase in *β*-carotene and the existing cyanobacteria pigments (echinenone, zeaxanthin). These suggest a remarkable increase in primary production in Zone II compared to Zone I. The appearance of other colonial cyanobacteria (cantaxanthin) and most importantly the appearance of oscillaxanthin indicate the intensive presence of cyanobacteria in this zone. Oscillaxanthin is mostly attributed to filamentous cyanobacteria *Planktothrix rubescens*, which was first observed in the lake in 1825, a period not included in our dataset. In our core, dominance of this species occurs from 37 cm to 27 cm with a peak at 32 cm. Its quantities before this part of the core were probably not high enough to be detected. The CD/TC ratio decreases, while the 430:410 ratio increases gradually as in Zone I (Fig. 4b).

The third group of PC1 scores is comprised of samples from 27 to 18 cm (Zone III), with higher scores for pigments specific to various green algae species and diatoms (lutein, diadinoxanthin, diatoxanthin), as well as to cyanobacteria species' (zeaxanthin, cantaxanthin) (Fig. 5). This zone is marked by a different trend in pigment composition. There is an alternation between oscillaxanthin and myxoxanthophyll. After an oscillaxanthin decrease, there is a subsequent increase in myxoxanthophyll (Fig. 4a). At this point *β*-carotene, echinenone, zeaxanthin, and oscillaxanthin decrease, which contrasts with an increase in myxoxanthophyll and cantaxanthin. This indicates a shift from filamentous to other colonial cyanobacteria species. There is also an increasing trend of asthaxanthin here typically indicating zooplankton grazing starting at 27 cm and right after oscillaxanthin decreases. Pheophorbide *α* that is also associated to zooplankton grazing increases at this point. The zooplankton increase assumes higher availability of accessible phytoplankton since the presence of filamentous toxic cyanobacteria decreases. The CD/TC ratio stays constant showing a decrease towards to the top of this zone, while 430:410 ratio increases (Fig. 4a).

The fourth group of PC1 scores from 18 to top (Zone IV), separates higher scores for pigments specific to green algae, diatoms and cryptophytes (Chl *b*, fucoxanthin, alloxanthin), as well as pigments indicating zooplankton grazing (pheophorbide *α*, astaxanthin) (Fig. 5). Astaxanthin shows a strong negative correlation with oscillaxanthin and myxol-2'-1 associated with filamentous *Oscillatoria* and other colonial species. This indicates that favorable conditions for grazing are present in this phase. This zone shows a shift in the phototrophic community from less cyanobacteria (echinenone, zeaxanthin), especially the colonial forms (cantaxanthin, myxoxanthophyll), to more green algae chlorophytes, euglenophytes (Chl *b*, lutein and violaxanthin), cryptophytes (alloxanthin) and diatoms, dinoflagellates, chrysophytes (diadinoxanthin, diatoxanthin) (Fig. 4a). From 7 cm to the surface, there is a further increase of green algae (Chl *b*, violaxanthin) and diatoms,

dinoflagellates denoted by the appearance of fucoxanthin and an increase in the existing diadinoxanthin and diatoxanthin. Peridin, which is a very labile compound associated with some dinoflagellates, appears here as well. However, cyanobacteria are still present (zeaxanthin, echinenone, cantaxanthin). The CD/TC ratio increases, whereas the 430:410 ratio stays overall stable with higher fluctuations (Fig. 4b).

Seasonal chemical data analysis in the water column

In the epilimnion, oxygen levels stay rather stable throughout the examined period, with lower values in October, after the summer stratification production peak (Fig. 6a). TP and DIP show a decreasing trend, for both May and October, with a first significant decrease starting in 1990, a further decrease in 1996 and then in 2002 with a minimum value in 2005. DIN in May shows a maximum value in 1988. Since 1989, concentrations are fluctuating with higher values in 1994-1996 and 2005-2007. Minimum values are in 2011-2012. In October, values show the same pattern, although they are overall lower than in May. DIN/TP ratios remain stable with a high peak in 2005.

In the hypolimnion in May, dissolved oxygen remains constant throughout the examined period (Fig. 6a). However, in October oxygen levels drops significantly overall, with lower values after 2001. TP concentrations in May follow a similar pattern as in the epilimnion and suggest that the main changes occurred in the late 1980s, and then in 1996 and 2002, with a minimum value in 2005. In October, TP concentrations start to decrease significantly since 1996, with a minimum in 2005. DIP in May shows a first decrease in 1990, then in 1996, and further in 2002 with minimum values in 2005 and after 2008. In October, the first significant decrease starts in 1996 with minimum values since 2002. DIN do not show significant changes for the examined period, however concentrations in May are higher than in October. DIN/TP ratios remain constant overall with a significant peak in 2005.

Fig. 6b shows the oxygen and temperature vertical profile in 2005, where we see a shift in nutrient levels (peak in DIN/TP ratios). The profile indicates a negative heterograde oxygen curve of a highly productive lake with a minimum in the metalimnion. At the end of February, holomixis is inferred by the homogenous vertical distribution of oxygen and temperature (93% of oxygen saturation). In August, oxygen distribution is variable, with high oxygen levels in the epilimnion (10.1 mg L^{-1}) at supersaturation (123 %) due to the photosynthetic activity of the rich algal biomass. In the metalimnion, oxygen concentration decreases drastically (3 mg L^{-1}) at 30% saturation by biological oxidation of the abundant OM from the

epilimnion. Oxygen levels increase in the upper hypolimnion (5.2 mg L^{-1} concentration, 45 % saturation) and decrease further to reach depletion above the sediments (0.3 mg L^{-1} concentration, 2 % saturation). In October, the metalimnion is incorporated in the epilimnion and below this level there is steep temperature gradient. Oxygen levels follow the same pattern due to continuous primary productivity in the epilimnion and decomposition of organic matter in the hypolimnion, which lead to a persistent oxygen depletion at the bottom water (0.2 mg L^{-1} concentration, 2 % saturation).

Discussion

Phytoplankton community variability in Lake Morat

Biological and physicochemical sediment proxies observed in Lake Morat provide evidences of the main phytoplankton community changes in the studied period. Radionuclide profiles indicate continuous sedimentation, suggesting that sediment mixing by physical processes or bioturbation were minor. Based on the petrophysical and chemical properties of the sediments, sequences show a rather stable sediment matrix. Hence, the trophic state of the lake reflects nutrients fluxes and lake internal processes clearly. Sediment pigment analysis allowed the discrimination of four phases of biomass production and phytoplankton community variability over the past 90 years:

Initial conditions prior to increased eutrophication (Zone I: AD 1924-1937)

In this zone, specific carotenoids reveals the presence mainly of green algae chlorophytes, euglenophytes (lutein) and diatoms, dinoflagellates, chrysophytes (diadinoxanthin), as well as less abundant cyanobacteria (echinenone, zeaxanthin). The 430:410 ratio decreases indicating the presence of more chlorophyll derivatives and less chlorophyll *α* in the sediments, likely caused by increasing oxygen levels (Dreßler et al. 2007). CD/TC ratio increases indicating higher content of CD than of TC, and thus a better trophic state with less cyanobacteria. As mentioned, the CD/TC ratio can serve as an index of the trophic status of the lakes based on the variations of total pigment concentrations. However, pigment degradation could also be responsible for the formation of CD/TC ratios in the sediments. Swain (1985) suggested that the CD/TC ratio is mostly determined by the phytoplankton community composition in meso-eutrophic lakes rather than by the preservation conditions. In Lake Morat, based on the stable

sediment matrix with stable sedimentation rates and constant anoxic conditions during stratification, as well as the comparison of the index with the chlorophyll and specific carotenoids concentrations throughout the core (Fig. 4a, b), the CD/TC ratio can reflect adequately trophic state changes. *In situ* measurements of phytoplankton conducted by Rivier (1936) during the same period coincide with specific carotenoids observations. Rivier revealed abundance of green algae species and diatoms, as well as the presence of cyanobacteria blooms including *Planktothrix rubescens*. However, their abundance must have been significantly low, as they are absent from the pigment distribution in this zone. *In situ* measurements of phosphorous (~10-15 μg L^{-1}), match with our primary production observations. According to pigment PCA scores (Fig. 5) and overall distribution of pigments along the core (Fig. 4), this zone reveals low pigment concentrations and low phytoplankton community variability.

Increasing eutrophication phase (Zone II: AD 1937-1970)

In this zone, pigment distributions increase abruptly, which indicates an overall increase in lake primary production. This response coincides with the extended hydrology works in the area, which affected the agricultural occupation (Magny et al. 2005), and increased nutrient inputs in the lake. Similar responses were also observed in the two surrounding lakes, Lake Biel (Santschi and Schindler 1977), and Lake Neuchatel (Liechti 1994). The change in the primary production is indicated by an increase in Chl *α*, *β*-carotene and pheophytin *α*, in carotenoids specific to green algae, diatoms, dinoflagellates (lutein, diatoxanthin, diadinoxanthin), as well as by a pronounced increase in cyanobacteria pigments (echinenone, zeaxanthin). Carotenoids that mark the presence of *Planktothrix rubescens* (oscillaxanthin) and other filamentous cyanobacteria (myxoxanthophyll, cantaxanthin, myxol-2'-1) also appear (Fig. 4a). *P. rubescens* are R-strategists, not favored by hypertrophic conditions but mostly mesotrophic to eutrophic (Konopka 1982). They colonize mainly the thermocline, where light and nutrient availability is high. Their dominance appears mainly from AD 1954-1970 (37-27 cm, with concentrations up to 800 nmol g^{-1} OM), which can be characterized as a gradually increasing eutrophication phase. Such episodic occurrences of *P. rubescens* have been also observed in other lakes in similar trophic phases (Legnani et al. 2005).

Intensive eutrophication phase (Zone III: AD 1970-1983)

In this part, PC1 scores change indicating a shift to less toxic cyanobacteria (Fig. 5). The pigment profile reveals a decline of *P. rubescens* (oscillaxanthin) and other toxic colonial cyanobacteria (myxol-2'-1) in AD 1970, accompanied by the appearance of zooplankton grazing (astaxanthin, pheophorbide *α*) (Fig. 4a). We consider increased nutrient levels, low light availability or temperature changes as possible explanations for *P. rubescens* decline giving space to other cyanobacteria species to develop. Our results support the hypothesis that the trophic state is important for *P. rubescens* dominance and that it is characterized by meso to eutrophic conditions. This agrees with studies in other lakes, Lake Bourget (Jacquet et al. 2014), and Lake Mondsee (Dokulil and Teubner 2012). This period coincides with the peak of phosphorous inputs into the lake, reaching 150 µg L^{-1} (Liechti 1994). The 430:410 ratio indicates a further decrease in oxygen levels in this part and the CD/TC ratio suggests mainly an unchanged trophic state, with remaining high presence of blue-green algae.

Restoration phase (Zone IV: AD 1983-2014)

This phase is marked by the restoration measures taken to reduce phosphorous inputs. We observe a further change in the phototrophic community composition with higher PC1 scores for green algae (Fig. 5). In pigment concentrations (Fig. 4a), we see a shift from cyanobacteria dominance to green algae (lutein, violaxanthin), cryptophytes (alloxanthin), diatoms, dinoglagellates, chrysophytes (diadinoxathnin, fucoxanthin, diatoxanthin). Pheophorbide *α* and astaxanthin, which began increasing in AD 1970, increase further at this point. This indicates dominance of less toxic algae. Nevertheless, cyanobacteria are still present but less abundant (echinenone, zeaxanthin, cantaxanthin). These results are consistent with the only study on the phytoplankton community composition in the lake during this period (Guthruf et al. 2009). It is reported that from 1999 to 2007 mainly diatoms, followed by cryptophytes, dominate algal biomass. Cyanobacteria are also present with a peak in 2005-2006 consisting mainly of *Microcystis aeruginosa*, which coincides with the peak in the DIN/TP ratio in the same year. These match the occurrence of higher values in cantaxanthin, zaxanthin, *β*-carotene, in our fossil record at 3-4 cm (Fig. 4a). *Microcystis* blooms have been shown to be N limited (Tsukada et al. 2006), which indicates an immediate response of algal composition to nutrient fluctuations in Lake Morat. Guthruf at al. report that *P. rubescens* is also present but only sporadically and at low biomasses. However, fossil pigment stratigraphy suggests

absence of the cyanobacterium after AD 1970. This can be attributed to biological degradation in the water column. Studies have shown that zooplankton species have developed adaptive responses to co-exist with *P. rubescens* (Kurmayer and Jüttner 1999) and that certain eukaryotes including protists (e.g ciliates) are able to degrade the cyanobacterium and its toxin with the synergetic effect of specific bacteria (Dirren et al. 2017). Thus, the absence of the cyanobacterium in the fossil record under low biomasses can be justified. We see that overall high primary production persists, although with different algal composition. The CD/TC ratio increases suggesting a better trophic condition in this zone with higher presence of green algae and less cyanobacteria. The 430:410 ratio indicates the same oxygen conditions with the previous zone, however with higher fluctuations. These give a good match with the varve formation in the sediments associated with high algal biomass and low oxygen conditions in the lake. These findings agree with zoobenthos composition for the period from 1980-1998 in Lake Morat (Lang 2000). Lang's results indicated a slow improvement of benthic conditions for the examined period however, the main species found in 1998 were characteristic of a eutrophic lake.

Lake Morat responses to re-oligotrophication

Phytoplankton community variability of Lake Morat shows rapid transitions between contrasting states for the studied period. We observe consecutive phases of increasing primary production with variable phytoplankton composition. Taking into account the short retention time of the lake (1.6 years), our pigment data together with available limnological data suggest that the lake reacts very quickly to nutrient concentration changes. We observe an immediate algal community response to changing conditions, while overall primary production response is slow. Excessive nutrient inputs can increase phytoplankton community variability and decrease significantly the effectiveness of lake management efforts (Cottingham et al. 2000). Studies suggest that multi-species assemblies can attain different equilibrium states for changing conditions with different responses (May 1977). Ecological system models predict different ecosystem responses to anthropogenic eutrophication that can create complex dynamical ecosystem responses and regime shifts in lakes (Scheffer et al. 2001; Scheffer and Carpenter 2003).

While nutrient increase usually leads to rapid ecosystem response, nutrient decrease often does not lead to immediate and complete reversal to the initial state (Sas 1989). Eutrophic lakes, according to their response to reduced P input loadings alone, may follow different

recovery trajectories. Explanations of a delayed or lack of response to nutrient reductions, usually suggest P recycling from sediments (Carpenter et al. 1999). Concentrations of TP in Lake Morat (Fig. 6a), indicate that a major decline in TP occurred in 1990, a few years after the initiation of phosphorous reduction efforts, and then again in 1996, 10 years after the initiation of restoration measures. DIP concentrations in the hypolimnion indicate recycling of inorganic forms of phosphorous from the sediments until 2002, 16 years after the initiation of the restoration measures in 1986. This agrees with previous findings on lakes' P recovery schemes following nutrient reduction (Sas 1989; Jeppesen et al. 2005).

Nonetheless, we do not observe any significant decrease in biomass production throughout restoration period continuing until today. Total algal biomass stays unchanged with different algal composition. Re-oligotrophication schemes of other deep lakes have been reported to follow convoluted recovery pathways with a response time from 10 to 30 years, usually with a decline in biomass (Anderson et al. 2005; Jeppesen et al. 2005). However, similar responses with a hysteresis of phytoplankton biomass reduction and with complex species composition has been also observed in other lakes (Dokulil and Teubner 2005; Grüneberg et al. 2011). In Lake Geneva phytoplankton responses during P reduction in the 1990s showed higher seasonal phytoplankton biomass in early spring due to warmer years (Anneville et al. 2002). This coupled with overall P decrease led to an early P depletion of the productive layer that created a distinctive vertical separation between algae and their resources. This can lead to an algae species adaptation, expanding the productive zone (Reynolds 1997). Our pigment data accord with these findings (Fig. 4a). After minimum pigment concentrations around 1983, we see a first smaller increase in the 1990s, followed by a further increase in the 2000s. This is also confirmed by *in situ* phytoplankton measurements in the same period (Guthruf et al. 2009). Nonetheless, comparing the present algae composition with the initial composition prior to increased eutrophication, we suggest that water quality will improve. Recent development of phytoplankton composition in Lake Morat is likely to be driven by the vertical P distribution in the water column. Hence, further and longer decrease of P inputs could lead to a re-adaptation of algae species and an eventual decrease of total algal biomass.

Conclusions

Sedimentary biological and physicochemical proxies used in Lake Morat allow us to identify four main phytoplankton community shifts over the past 90 years. Pigment profiles accurately show the response of the phytoplankton community to intense anthropogenic stresses in the 20th century, and during the restoration period that followed. Overall, we observe that cyanobacteria and in particular *Planktothrix* seem to play an important role in phytoplankton community shifts and determining separation in the samples.

The oldest part of the core (AD 1924-1937) allows for the observation of pigment profiles and physicochemical proxies' levels before the intense eutrophication phase. In the following years (AD 1937-1983), the lake suffered from high primary production characterized by less desirable species, occurrence of pronounced oxygen depletion and overall degradation of its quality. *Planktothrix rubescens* filamentous cyanobacterium, which was first observed in the lake since the 19th century, became more abundant in this part, dominating algae community species together with other cyanobacteria. Since AD 1983, during the re-oligotrophication period, pigment concentrations suggest a new trend marked by a shift in the phototrophic community to more green algae while cyanobacteria remain present, but at decreased concentrations. In this period, contemporary limnological data revealed a delayed total phosphorous decrease of 10-16 years after the beginning of the restoration measures in 1986, due to P recycling from the sediments. Despite the drastic reduction of phosphorous concentrations, biomass levels stay relatively stable, yet algal composition changes. Overall, we see that algal community responds very fast to nutrient changes, however total biomass production stays unchanged. Based on pigment concentrations, together with nutrient levels during the restoration period, we consider species adaptation to a P depleted productive layer as a possible explanation of persistent total algal biomass. Nutrient reduction efforts may lead to natural nutrient levels in the lake, however will not necessarily lead to initial reference trophic conditions.

This study highlights the significant role of paleolimnological data for a more holistic, synthetic approach for past trophic state reconstructions, as well as the clarification of re-oligotrophication patterns and processes in eutrophicated lakes. Multidisciplinary sediment data can successfully extend the limited timescale covered by contemporary limnological datasets and help us understand lake responses during the eutrophication and re-oligotrophication periods.

Acknowledgements

The University of Geneva and the Hans Sigrist Foundation funded this research. We thank the Institute of Ecosystem Study in Pallanza, Italy for hosting the HPLC analysis and the Department of Earth Sciences at the University of Bern for XRF scanning, under the supervision of Dr. Hendrik Vogel. We thank Prof. Dr. Daniel Ariztegui and Dr. Camille Thomas for their help with CN analysis. Many thanks to Tiago André Adriao Silva and Philippe Arpagaus for their help in the field. The BENEFRI group led by the cantons of Bern, Fribourg, Neuchâtel and Vaud for providing the lake limnological data. Special thanks to Prof. Dr. Martin Grosjean for commenting on the manuscript. We would also like to acknowledge journal reviewers for their constructive comments and editorial work.

References

Anderson J, Jeppesen E, Søndergaard M (2005) Ecological effects of reduced nutrient loading (oligotrophication) on lakes: an introduction. Freshw Biol 50:1589–1593

Anneville O, Ginot V, Angeli N (2002) Restoration of Lake Geneva: Expected versus observed responses of phytoplankton to decreases in phosphorus. Lakes Reserv Res Manag 7:67–80

Appleby P (2001) Chronostratigraphic techniques in recent sediments. In: Last W, Smol J (eds) Tracking Environmental Change Using Lake Sediments. Springer Netherlands, Dordrecht, pp 171–203

Battarbee RW, Anderson NJ, Jeppesen E, Leavitt PR (2005) Combining palaeolimnological and limnological approaches in assessing lake ecosystem response to nutrient reduction. Freshw Biol 50:1772–1780

BENEFRI (2017) Les 3 Lacs: La surveillance de l'état qualitatif des lacs de Morat, Neuchâtel et Bienne. http://www.die3seen.ch/

Carpenter SR, Ludwig D, Brock WA (1999) Management of Eutrophication for Lakes Subject to Potentially Irreversible Change. Ecol Appl 9:751–771

Cottingham KL, Rusak JA, Leavitt PR (2000) Increased ecosystem variability and reduced predictability following fertilisation: Evidence from palaeolimnology. Ecol Lett 3:340–348

Davaud E (1976) Contribution à l'étude géochimique et sédimentologique des dépôts lacustres récents (Lac de Morat, Suisse). Thèse n° 1475, Fac. Sci. Université de Genève, 129 p.

Dean WE (1974) Determination of carbonate and organic matter in calcareous sediments and sedimentary rocks by loss on ignition; comparison with other methods. J Sediment Res 44:242–248

Dirren S, Pitsch G, Silva MOD, Posch T (2017) Grazing of Nuclearia thermophila and Nuclearia delicatula (Nucleariidae, Opisthokonta) on the toxic cyanobacterium Planktothrix rubescens. Eur J Protistol 60:87–101

Dokulil MT, Teubner K (2012) Deep living Planktothrix rubescens modulated by environmental constraints and climate forcing. Hydrobiologia 698:29–46

Dokulil MT, Teubner K (2005) Do phytoplankton communities correctly track trophic changes? An assessment using directly measured and palaeolimnological data. Freshw Biol 50:1594–1604

Dreßler M, Hübener T, Görs S, et al (2007) Multi-proxy Reconstruction of Trophic State,

Hypolimnetic Anoxia and Phototrophic Sulphur Bacteria Abundance in a Dimictic Lake in Northern Germany over the past 80 Years. J Paleolimnol 37:205–219

EAWAG (1960) Der Murtensee. Sein gegenwärtiger chemisch-biologischer Zustand. Die Herkunft der eutrophierenden Stoffe. Seesanierung – Schutz vor Verunreinigung. Gesamtbericht über die von der Eawag in den Jahren 1954/1955 durchgeführten Erhebungen. Zürich, 59 p.

Grüneberg B, Rücker J, Nixdorf B, Behrendt H (2011) Dilemma of Non-Steady State in Lakes - Development and Predictability of In-Lake P Concentration in Dimictic Lake Scharmützelsee (Germany) after Abrupt Load Reduction. Int Rev Hydrobiol 96:599–621

Guilizzoni P, Bonomi G, Galanti G, Ruggiu D (1983) Paleolimnology: Relationship between sedimentary pigments and primary production: evidence from core analyses of twelve Italian lakes. In: Meriläinen J, Huttunen P, Battarbee RW (eds) Hydrobiologia. Kluwer Academic Publishers, The Hague, Netherlands, pp 103–106

Guilizzoni P, Lami A (2002) Paleolimnology: Use of Algal Pigments as Indicators. In: Bitton G (ed) Encyclopedia of Environmental Microbiology. John Wiley & Sons, Inc., New York, pp 2306–2317

Guilizzoni P, Lami A, Marchetto A (1992) Plant pigment ratios from lakes sediments as indicators of recent acidification in alpine lakes. Limnol Oceanogr 37:1565–1569

Guthruf K, Maurer V, Pokorni B, Zeh M (2009) Le développement du phytoplancton et du plancton de crustacés (Brienzersee, Thunersee, Murtensee - Lac de Morat, Lac de Neuchâtel, Bielersee). Rapport. Édité par l' AWA, SEN, SCPE. Berne, 112 p.

Heiri O, Lotter AF, Lemcke G (2001) Loss on ignition as a method for estimating organic and carbonate content in sediments: reproducibility and comparability of results. J Paleolimnol 25:101–110

Hertzberg S, Liaaen-Jensen S, Siegelman HW (1971) The carotenoids of blue-green algae. Phytochemistry 10:3121–3127

Jacquet S, Kerimoglu O, Rimet F, et al (2014) Cyanobacterial bloom termination: the disappearance of Planktothrix rubescens from Lake Bourget (France) after restoration. Freshw Biol 59:2472–2487

Jenny J-P, Francus P, Normandeau A, et al (2016) Global spread of hypoxia in freshwater ecosystems during the last three centuries is caused by rising local human pressure. Glob Chang Biol 22: 1481-1489

Jeppesen E, Søndergaard M, Jensen JP, et al (2005) Lake responses to reduced nutrient loading – an analysis of contemporary long-term data from 35 case studies. Freshw Biol

50:1747–1771

Kaste JM, Norton SA, Hess CT (2002) Environmental chemistry of beryllium-7. Mineral Soc Am 50:271–289

Koinig KA, Shotyk W, Lotter AF, et al (2003) 9000 years of geochemical evolution of lithogenic major and trace elements in the sediment of an alpine lake - the role of climate, vegetation, and land-use history. J Paleolimnol 30:307–320

Konopka A (1982) Physiological ecology of a metalimnetic Oscillatoria rubescens population. Limnol Oceanogr 27:1154–1161

Kurmayer R, Jüttner F (1999) Strategies for the co-existence of zooplankton with the toxic cyanobacterium Planktothrix rubescens in Lake Zurich. J Plankton Res 21:659–683

Lami A, Guilizzoni P, Marchetto A (2000) High resolution analysis of fossil pigments, carbon, nitrogen and sulphur in the sediment of eight European Alpine lakes: the MOLAR project. J Limnol 59:15–28

Lami A, Niessen F, Guilizzoni P, et al (1994) Palaeolimnological studies of the eutrophication of volcanic Lake Albano (Central Italy). J Paleolimnol 10:181–197

Lang C (2000) Etat trophique du lac de Morat indiqué par le zoobenthos: tendance 1980-1998. Rev suisse Zool 107:233–243

Leavitt P, Hodgson D (2001) Practical methods for analysis of sedimentary pigments. In: JP S, Birks H, Last W (eds) Developments in Palaeoenvironmental Research. Kluwer Academic Publishers, Dordrecht, The Netherlands, pp 295–325

Leavitt PR (1993) A review of factors that regulate carotenoid and chlorophyll deposition and fossil pigment abundance. J Paleolimnol 9:109–127

Legnani E, Copetti D, Oggioni A, et al (2005) Planktothrix rubescens' seasonal dynamics and vertical distribution in Lake Pusiano (North Italy). J Limnol 64:61–73

Liechti P (1994) L'état des lacs en Suisse: Le Lac de Morat. Rapport, Cahier de l'environnement n° 237. Édité par l'Office fédéral de l'environnement, des forêts et du paysage OFEFP. Berne, 163 p.

Loizeau J-L, Arbouille D, Santiago S, Vernet J-P (1994) Evaluation of a wide range laser diffraction grain size analyser for use with sediments. Sedimentology 41:353–361

Magny M, Peyron O, Bégeot C, Guiot J (2005) Quantitative reconstruction of mid-Holocene climatic variations in the northern Alpine foreland based on Lake Morat (Swiss Plateau) and Lake Annecy (French Pre-Alps) data. Boreas 34:434–444

Mantoura RFC, Llewellyn CA (1983) The rapid determination of algal chlorophyll and carotenoid pigments and their breakdown products in natural waters by reverse-phase

high-performance liquid chromatography. Anal Chim Acta 151:297–314

Mardsen MW (1989) Lake restoration by reducing external phosphorus loading: the influence of sediment phosphorus release. Freshw Biol 21:139–162

May RM (1977) Thresholds and breakpoints in ecosystems with a multiplicity of stable states. Nature 269:471–477

Meyers PA, Benson L V (1988) Sedimentary biomarker and isotopic indicators of the paleoclimatic history of the Walker Lake basin, western Nevada. Org Geochem 13:807–813

Müller B, Schmid M (2009) Bilans du phosphore et de l'oxygène dans le lac de Morat. Rapport. Eawag - Institut fédéral suisse des sciences et technologies aquatiques. Kastanienbaum, 42 p.

Oksanen J, Blanchet GF, Friendly M, et al (2017) Community Ecology Package "vegan". R package version 2.4-3

R Core Team (2015) R: A language and environment for statistical computing.

Reynolds S (1997) Vegetation processes in the pelagic: A model for ecosystem theory. Ecology Institute, Oldendorf

Rivier O (1936) Recherche hydrobiologique sur le Lac de Morat. Bull la Société Neuchâteloise des Sci Nat 61:66

Roy S, Llewellyn C, Egeland ES, Johnsen G (eds) (2011) Phytoplankton Pigments. Cambridge University Press, Cambridge

Santschi PW, Schindler PW (1977) Chemical and geochemical studies of Lake Biel I. A mass balance for Lake Biel and its implications for the rates of erosion of the drainage area. Schweizerische Zeitschrift für Hydrol 39:182–200

Sas H (1989) Lake restoration by reduction of nutrient loading: expectations, experiences, extrapolations. Academia Verlag Richarz, Sankt Augustin

Scheffer M, Carpenter S, Foley JA, et al (2001) Catastrophic shifts in ecosystems. Nature 413:591–596

Scheffer M, Carpenter SR (2003) Catastrophic regime shifts in ecosystems: linking theory to observation. Trends Ecol Evol 18:648–656

Schindler DW (2006) Recent advances in the understanding and management of eutrophication. Limnol Oceanogr 51:356–363

Schnurrenberger D, Russell J, Kelts K (2003) Classification of lacustrine sediments based on sedimentary components. J Paleolimnol 29:141–154

Smith VH, Schindler DW (2009) Eutrophication science: where do we go from here? Trends

Ecol Evol 24:201–207

Smol JP (2010) The power of the past: using sediments to track the effects of multiple stressors on lake ecosystems. Freshw Biol 55:43–59

Swain EB (1985) Measurement and interpretation of sedimentary pigments. Freshw Biol 15:53–75

Swisstopo (2016) Swiss Federal Office of Topography. https://www.swisstopo.admin.ch

Tsukada H, Tsujimura S, Nakahara H (2006) Effect of nutrient availability on the C, N, and P elemental ratios in the cyanobacterium Microcystis aeruginosa. Limnology 7:185–192

von Gunten L, Grosjean M, Kamenik C, et al (2012) Calibrating biogeochemical and physical climate proxies from non-varved lake sediments with meteorological data: methods and case studies. J Paleolimnol 47:583–600

Yacobi YZ, Mantoura RFC, Llewellyn CA (1991) The distribution of chlorophylls, carotenoids and their breakdown products in Lake Kinneret (Israel) sediments. Freshw Biol 26:1–10

Tables

Table 1 Morphological and limnological characteristics of Lake Morat (Liechti 1994)

Lake Morat (Switzerland)	**Lat. 46.907°, Long. 7.021°**
Lake elevation	429 m a.s.l.
Water surface	22.8 km^2
Max. depth	45 m
Average depth	23 m
Lake volume	0.53 km^3
Volume of hypolimnion (>10m)	0.34 km^3
Water retention time	1.54 years
Watershed surface	713 km^2
Income volume flow rate (Broye contribution 87%)	10.8 m^3 s^{-1}
Number of wastewater treatment plants (direct input)	1
Number of total wastewater treatment plants	32
Number of inhabitants	73,500

Figure captions

Fig. 1a Land use map of the catchment area, and its position within Switzerland (Swisstopo 2016). **b** Bathymetric map of the lake indicating the coring site.

Fig. 2 Sedimentological and geochemical proxy data of Lake Morat.

Fig. 3 Sediment chronology: ^{137}Cs and ^{210}Pb activity curves and CRS model ages.

Fig. 4a Pigment stratigraphy of chlorophylls, their derivatives and specific carotenoids. **b** Chlorophyll derivatives (CD), total carotenoids (TC), CD/TC and 430:410 ratios profiles. The red dashed lines mark the four separation zones as defined by the constrained cluster analysis.

Fig. 5 PCA bi-plot and clustering dendrogram of chlorophylls and specific carotenoids.

Fig. 6a Chemical data in the water column for May and October from 1986 to 2014 (TP: total phosphorous, DIP: dissolved inorganic phosphorous, DIN: dissolved inorganic nitrogen). **b** Vertical distribution of oxygen and temperature during the main seasonal phases in 2005.

Figures

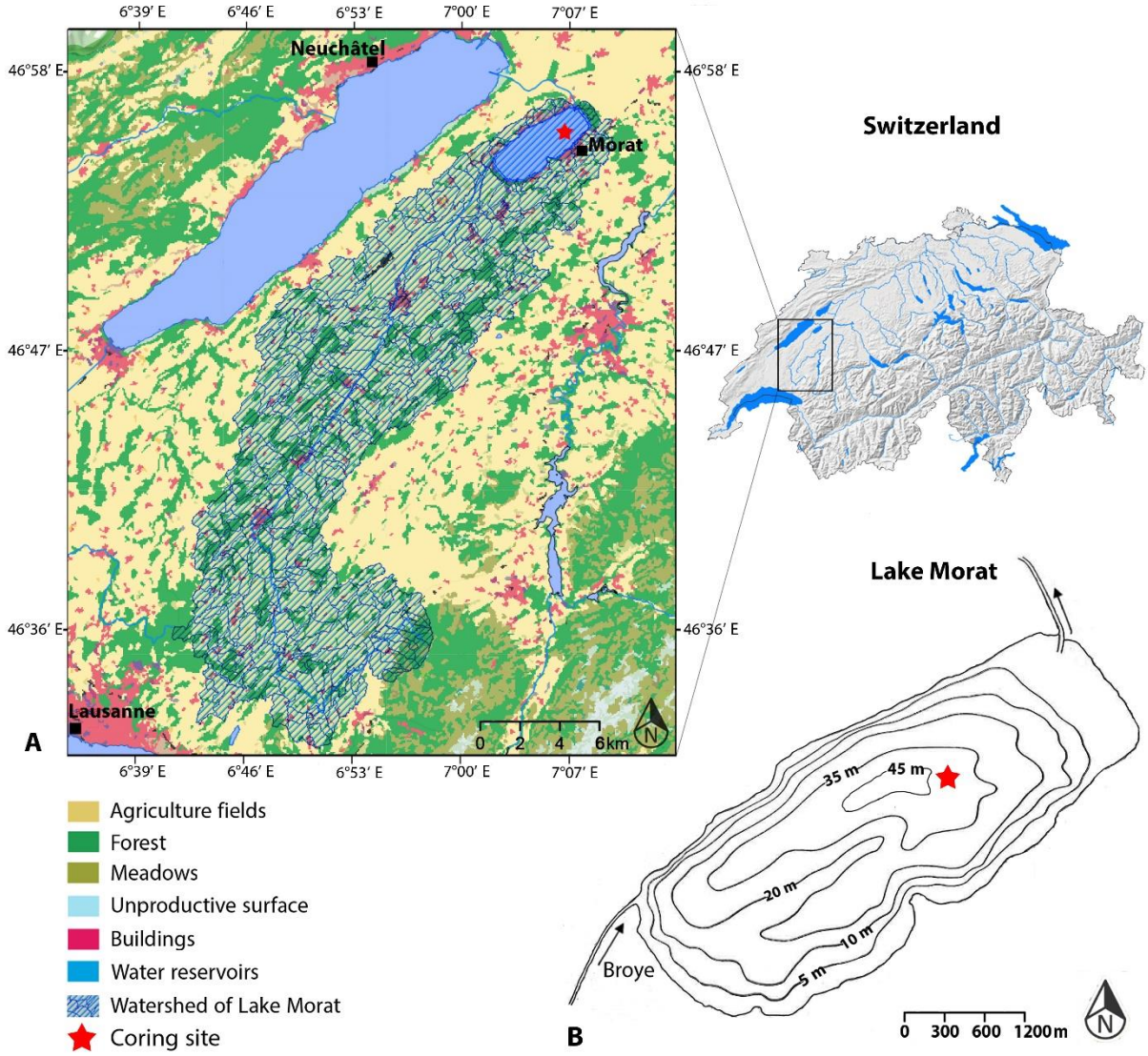

Fig. 1

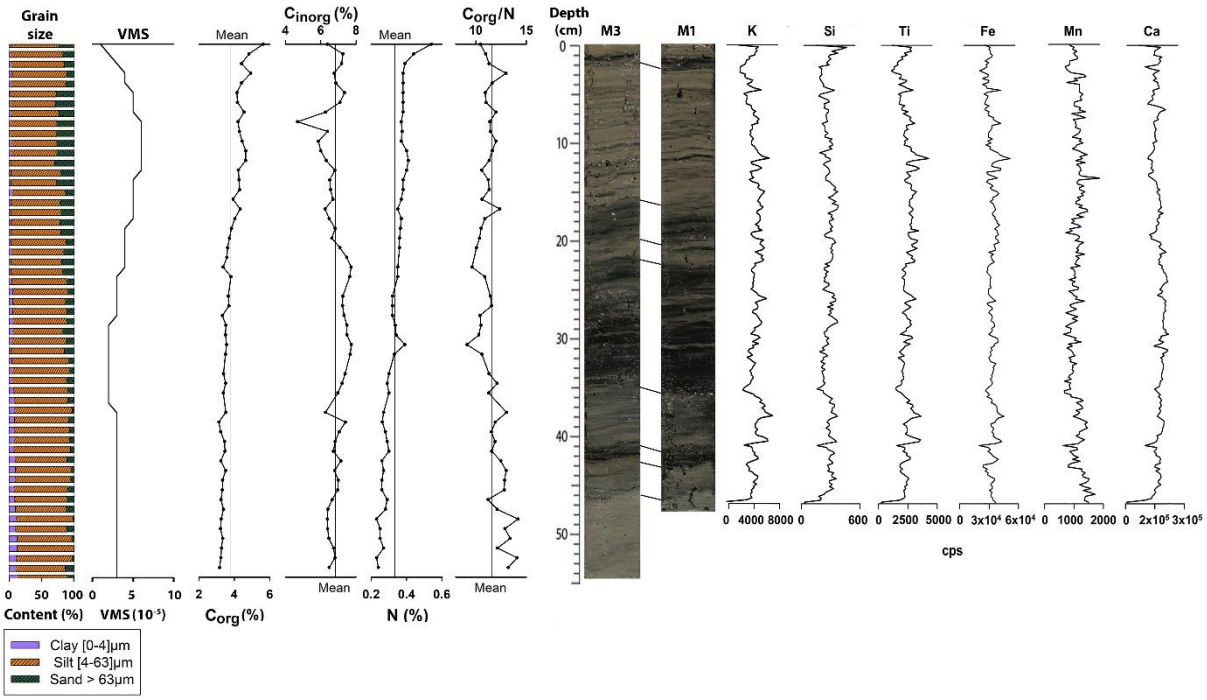
Grain size
VMS
Mean
Cinorg (%)
4 6 8
Mean
Corg/N
10 15
Depth (cm)
M3
M1
K
Si
Ti
Fe
Mn
Ca
0
10
20
30
40
50
0 50 100
Content (%)
0 5 10
VMS (10-5)
2 4 6
Corg (%)
Mean
0.2 0.4 0.6
N (%)
Mean
0 4000 8000
0 600
0 2500 5000
0 3x10⁴ 6x10⁴
0 1000 2000
0 2x10⁵ 3x10⁵
cps
Clay [0-4]µm
Silt [4-63]µm
Sand > 63µm

Fig. 2

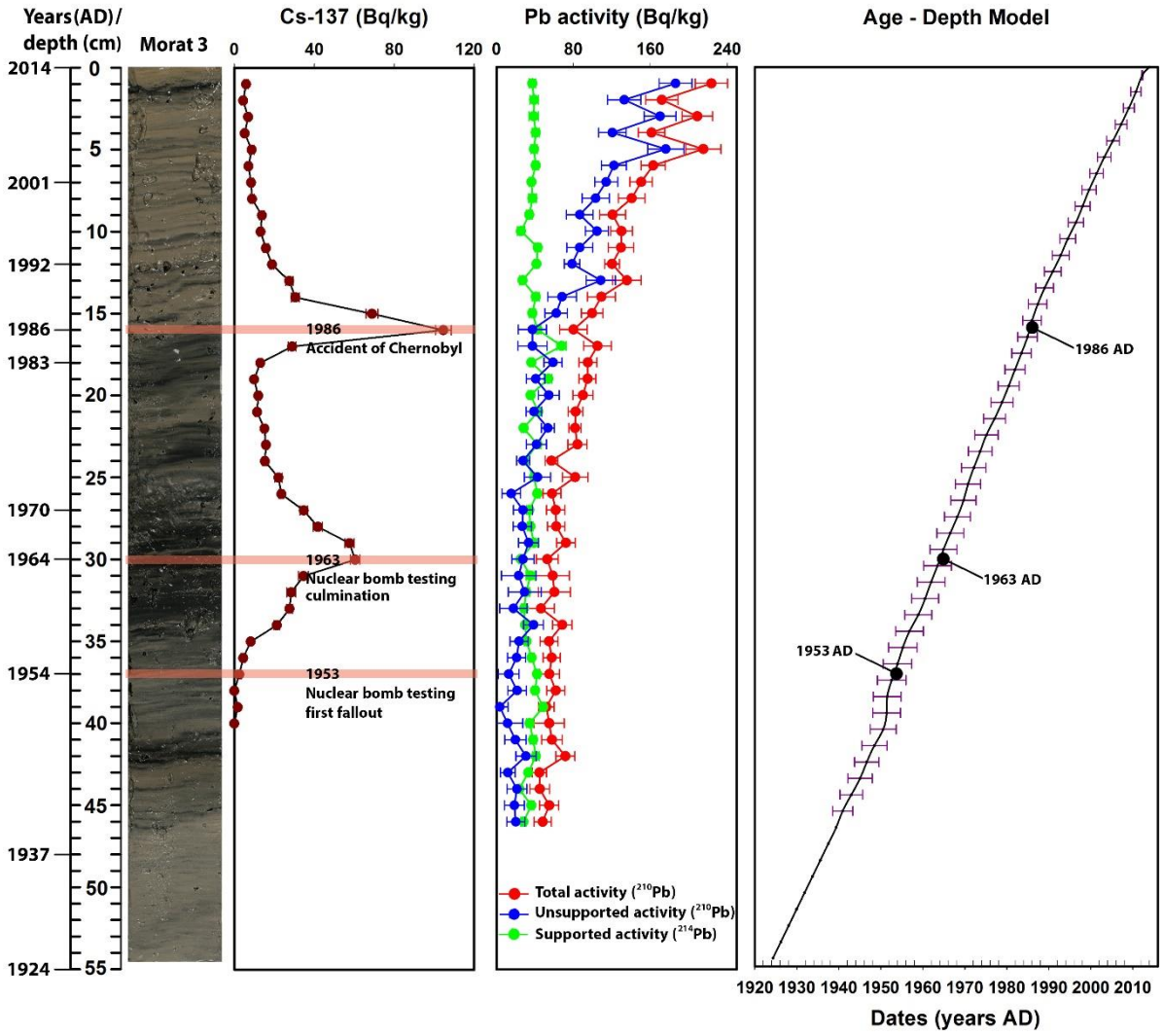
Years(AD)/
depth (cm)
Morat 3
Cs-137 (Bq/kg)
Pb activity (Bq/kg)
Age - Depth Model
1986
Accident of Chernobyl
1963
Nuclear bomb testing
culmination
1953
Nuclear bomb testing
first fallout
Total activity (210Pb)
Unsupported activity (210Pb)
Supported activity (214Pb)
1986 AD
1963 AD
1953 AD
Dates (years AD)

Fig. 3

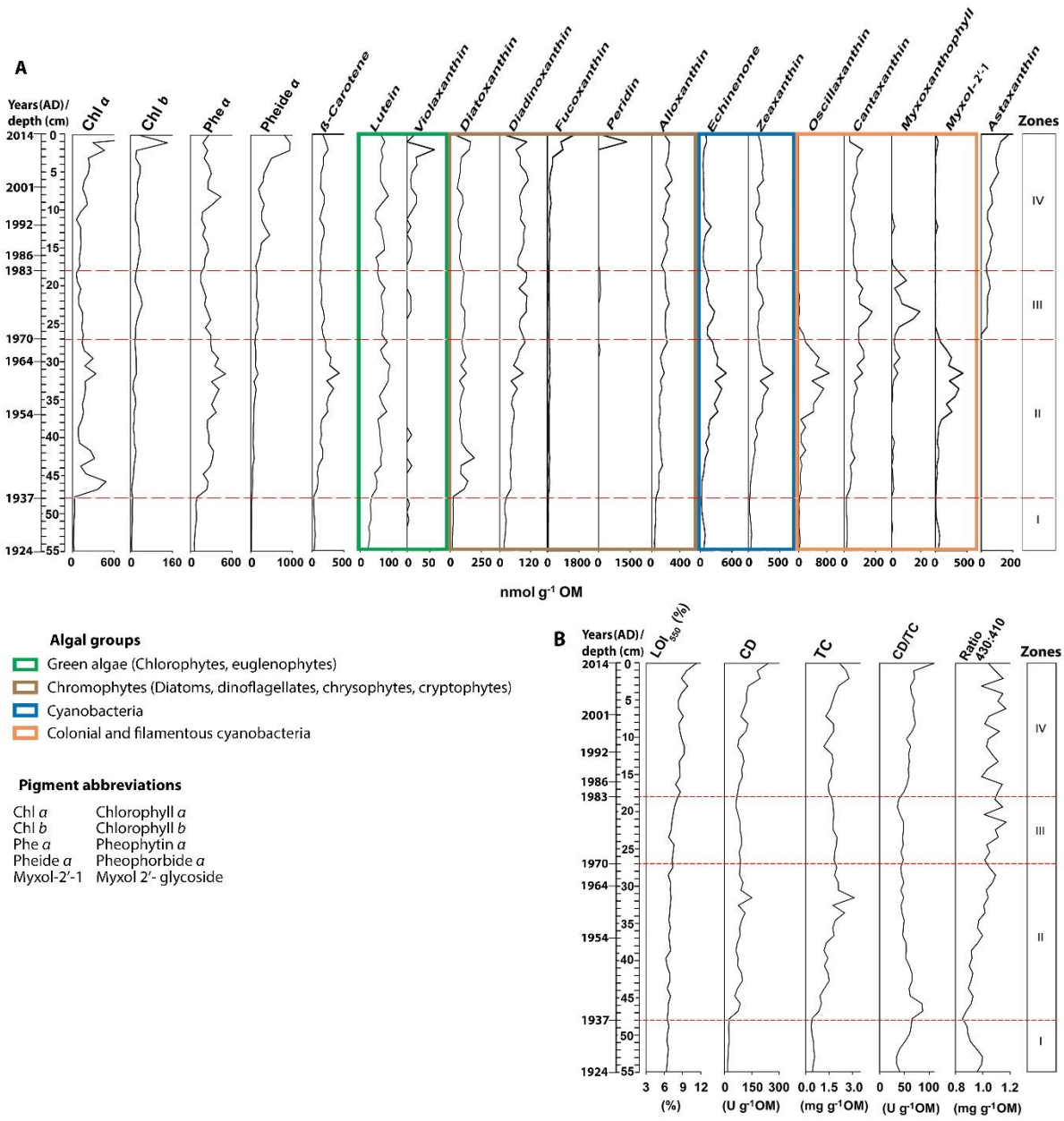
A
Years(AD)/ depth (cm)
Chl a
Chl b
Phe a
Pheide a
β-Carotene
Lutein
Violaxanthin
Diatoxanthin
Diadinoxanthin
Fucoxanthin
Peridin
Alloxanthin
Echinenone
Zeaxanthin
Oscillaxanthin
Cantaxanthin
Myxoxanthophyll
Myxol-2'-1
Astaxanthin
Zones
2014
2001
1992
1986
1983
1970
1964
1954
1937
1924
IV
III
II
I
nmol g-1 OM
Algal groups
Green algae (Chlorophytes, euglenophytes)
Chromophytes (Diatoms, dinoflagellates, chrysophytes, cryptophytes)
Cyanobacteria
Colonial and filamentous cyanobacteria
Pigment abbreviations
Chl a Chlorophyll a
Chl b Chlorophyll b
Phe a Pheophytin a
Pheide a Pheophorbide a
Myxol-2'-1 Myxol 2'- glycoside
B
Years(AD)/ depth (cm)
LOI550 (%)
CD
TC
CD/TC
Ratio 430:410
Zones
(%)
(U g-1OM)
(mg g-1OM)
(U g-1OM)
(mg g-1OM)

Fig. 4

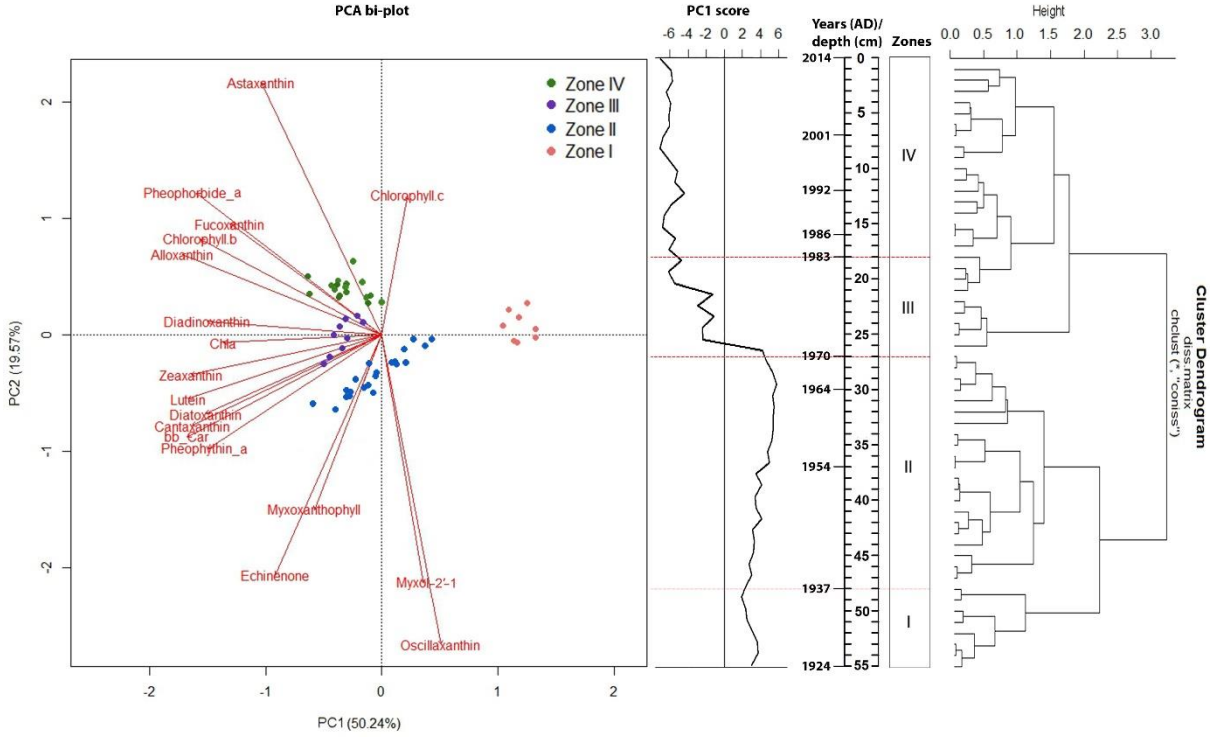
PCA bi-plot
PC1 score
Years (AD)/ depth (cm)
Zones
Height
Cluster Dendrogram
Zone IV
Zone III
Zone II
Zone I
Astaxanthin
Pheophorbide_a
Chlorophyll.c
Fucoxanthin
Chlorophyll.b
Alloxanthin
Diadinoxanthin
Chla
Zeaxanthin
Lutein
Diatoxanthin
Canthaxanthin
bb_Car
Pheophytin_a
Myxoxanthophyll
Echinenone
Myxol-2'-1
Oscillaxanthin
PC2 (19.57%)
PC1 (50.24%)
IV
III
II
I

Fig. 5

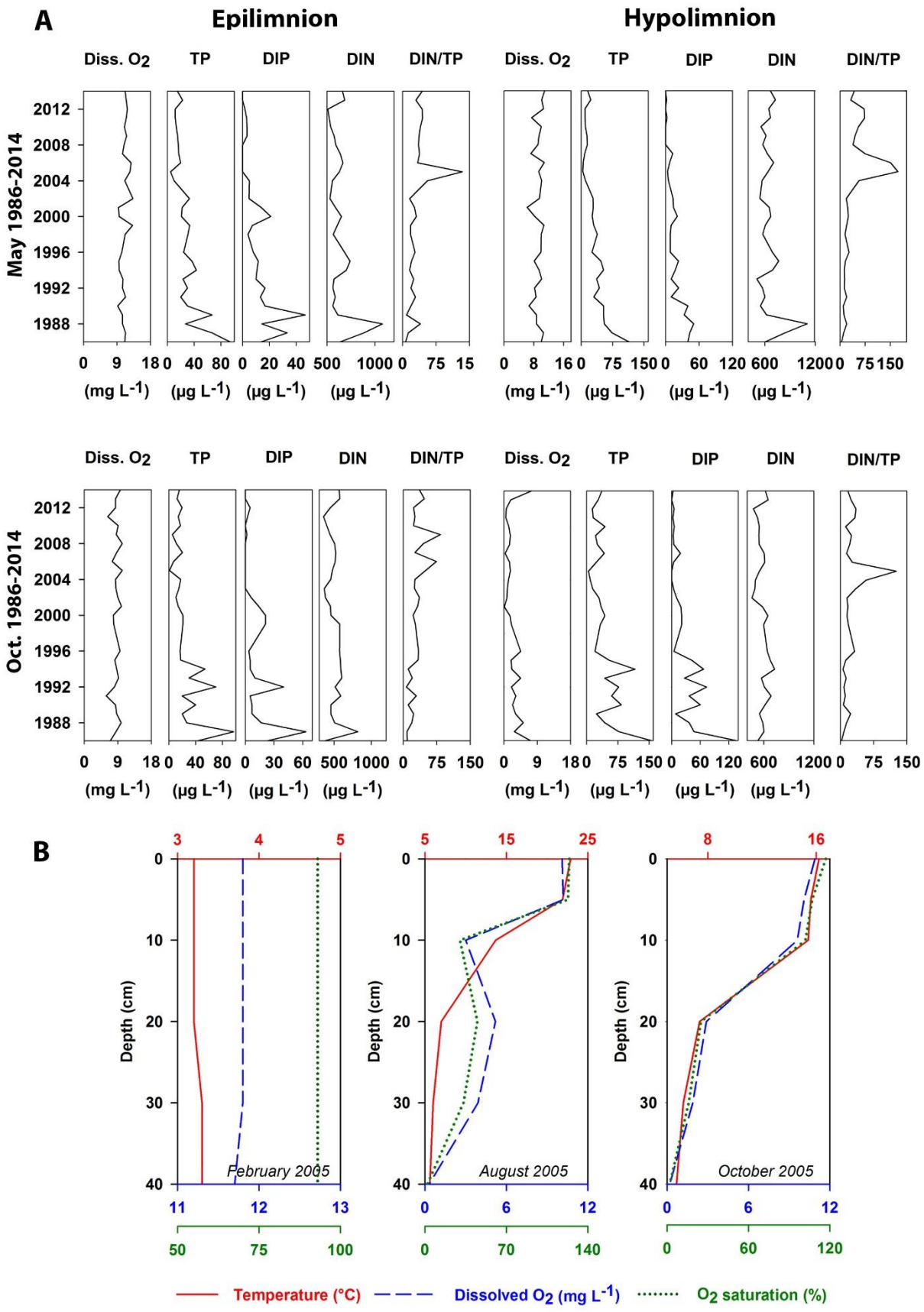
A
Epilimnion
Hypolimnion
Diss. O2
TP
DIP
DIN
DIN/TP
May 1986-2014
Oct. 1986-2014
2012
2008
2004
2000
1996
1992
1988
(mg L-1)
(µg L-1)
B
Depth (cm)
February 2005
August 2005
October 2005
Temperature (°C)
Dissolved O2 (mg L-1)
O2 saturation (%)

Fig. 6